Contribution from the Department of Chemistry,
University of California, Berkeley, California 94720

Effect of Packing Forces on the Geometry of the $[Ni(CN)_5]^{3-}$ Ion: Structures of $[Cr(NH_2CH_2CH_2CH_2NH_2)_3][Ni(CN)_5]\cdot 2H_2O$ and $[Cr(NH_3)_6][Ni(CN)_5]\cdot 2H_2O$. A Skew-Boat Conformation in a Six-Membered Metal Chelate Ring

FRANCES A. JURNAK and KENNETH N. RAYMOND*[1]

Received October 5, 1973 AIC30729F

The crystal and molecular structures of two salts containing the $[Ni(CN)_5]^{3-}$ anion have been determined at −80 and −10° from three-dimensional X-ray diffraction data collected by counter methods. Since both distorted trigonal-bipyramidal and square-pyramidal geometries of the $[Ni(CN)_5]^{3-}$ ion exist in the salt $[Cr(en)_3]_2[Ni(CN)_5]_2\cdot 3H_2O$, the question has remained as to whether the observed geometries correspond to discrete, stable structures or are artifacts of crystal packing forces. The geometry of the $[Ni(CN)_5]^{3-}$ anion in both salts reported here can be described as a regular square pyramid in which the apical Ni–C bond distance is considerably longer than the basal Ni–C bonds. In the $[Cr(tn)_3]^{3+}$ salt, the apical Ni–C distance is 2.140 (10) Å and the average basal Ni–C distance is 1.877 (9) Å; in the $[Cr(NH_3)_6]^{3+}$ salt, the apical and average basal Ni–C bond distances are 2.101 (9) and 1.877 (7) Å, respectively. The presence of the same $[Ni(CN)_5]^{3-}$ structure in the salts $[Cr(en)_3]_2[Ni(CN)_5]_2\cdot 3H_2O$, $[Cr(tn)_3][Ni(CN)_5]\cdot 2H_2O$, and $[Cr(en)_3]_2[Ni(CN)_5]_2\cdot 2H_2O$ is cited as evidence for the stereochemical rigidity of the square-pyramidal $[Ni(CN)_5]^{3-}$ ion, since the crystal packing forces differ substantially in detail from one salt to another. Average Cr–N bond distances for $[Cr(tn)_3]^{3+}$ and $[Cr(NH_3)_6]^{3+}$ are 2.096 (3) and 2.080 (4) Å, respectively. In the former cation, only two of the three six-membered rings have the expected chair conformation. The third ring has a conformation analogous to the twist or skew-boat form of cyclohexane. The average N–Cr–N angle for all rings is 89.7 (3)° and the average Cr–N–C angle is 120.7 (4)° in the chair and 116.6 (2)° in the skew-boat conformers. A comparison of all structural examples of the chair geometry in 1,3-propanediamine chelate rings is discussed. The dihedral angle between the planes containing the N–C bonds in the twist conformer is 79.0°. Tris(1,3-propanediamine)chromium(III) pentacyanonickelate(II) dihydrate, $[Cr(tn)_3][Ni(CN)_5]\cdot 2H_2O$, forms deep red crystals in the orthorhombic space group *Pbca* with $a = 23.442$ (7), $b = 13.239$ (4), and $c = 14.352$ (6) Å at −80°. For eight formula units in the cell the calculated density is 1.49 g/cm³ at −80°, which agrees well with that observed at 23°, 1.48 g/cm³. For 1671 independent reflections with $F^2 > 3\sigma(F^2)$ full-matrix least-squares refinement of positional and anisotropic thermal parameters converged to a final weighted R factor of 5.4%. The second salt, $[Cr(NH_3)_6][Ni(CN_5]\cdot 2H_2O$, crystallizes in the orthorhombic space group *Pcca* with eight formula units in a cell of dimensions $a = 23.102$ (10), $b = 11.529$ (3), and $c = 11.735$ (4) Å at −10°. The calculated (−80°) and observed (23°) densities are 1.61 and 1.60 g/cm³, respectively. Full-matrix least-squares refinement for 1090 independent reflections with $F^2 > \sigma(F^2)$ converged to $R = 4.7\%$. Room- and low-temperature data sets for $[Cr(tn)_3][Ni(CN)_5]\cdot 2H_2O$ are compared and the effect of isotropic crystal decomposition on structural information is discussed.

Introduction

Among the lower coordination numbers, five-coordinate complexes are unique in their stereochemical flexibility. Complexes are known with both of the highest symmetry geometries, trigonal bipyramidal (D_{3h}) and square pyramidal (C_{4v}), and a wide range of intermediate geometries.[2] However, there is to date only one d^8 complex which is known to exist in more than one static geometry.[2c] This is the $[Ni(CN_5]^{3-}$ ion as found in the crystalline salt $[Cr(en)_3]_2[Ni(CN)_5]_2\cdot 3H_2O$ (en = ethylenediamine).[3] In that salt the anion exists in two forms: a regular square-pyramidal geometry and a distorted trigonal-bipyramidal form. The differences in geometry (especially metal–ligand bond lengths) between the two anions in the salt would seem to indicate a large difference in the mode of bonding, yet the energy difference must be at most a few kilocalories per mole since the crystal environments of the two geometries are nearly the same. If the geometry of the $[Ni(CN)_5]^{3-}$ ion can convert from a trigonal-bipyramidal to a square-pyramidal form with little change in energy, the anion should exhibit changes in geometry from one salt to another as the packing forces change. If, on the other hand, these geometries correspond to relatively deep energy minima, crystal packing forces should not alter substantially the structure of the anion. In order to determine the geometry of $[Ni(CN)_5]^{3-}$ in several environments and to test the sensitivity of the geometry to crystal packing forces, we have prepared a number of salts of this complex anion. The cyanide stretching modes of vibration have been assigned for several environments of the $[Ni(CN)_5]^{3-}$ ion from Raman and infrared spectra and preliminary X-ray diffraction data.[4] We report here the crystal and molecular structures of the salts $[Cr(tn)_3][Ni(CN)_5]\cdot 2H_2O$ (tn = 1,3-propanediamine) and $[Cr(NH_3)_6][Ni(CN)_5]\cdot 2H_2O$.

Experimental Section

Preparations. $[Cr(tn)_3][Ni(CN)_5]\cdot 2H_2O$. To a solution containing 1.62 g of KCN and 1.00 g of $K_2Ni(CN)_4\cdot H_2O$ in 70 ml of H_2O was added, with stirring, a solution of 1.38 g of $[Cr(tn)_3]Cl_3$[5] in 50 ml of H_2O. The resultant clear, yellow-orange solution was cooled to 4°. After several hours the red crystalline product was collected by suction filtration, rapidly washed with a small portion of water and air-dried. The yield was approximately 70%. Weight loss of the crystalline product under vacuum at room temperature was 7.7%. Assuming loss of H_2O this corresponds to 2.08 mol of H_2O/mol of salt. The dried salt was then analyzed. *Anal.* Calcd for $NiCrN_{11}C_{14}H_{30}$: Ni, 13.44; Cr, 11.90; N, 34.26; C, 38.40; H, 4.2. Found: Ni, 13.46; Cr, 11.88; N, 34.83; C, 37.56; H, 4.6.

$[Cr(NH_3)_6][Ni(CN)_5]\cdot 2H_2O$. Crystals of the compound were

(1) Alfred P. Sloan Fellow, 1971–1973.

(2) (a) B. A. Frenz and J. A. Ibers, *Inorg. Chem.*, **11**, 1109 (1972). (b) B. A. Frenz and J. A. Ibers, "The Biennial Review of Chemistry, Chemical Crystallography," J. M. Robertson, Ed., Medical and Technical Publishing Co., Aylesburg, England, 1972, Chapter 2. (c) A five-coordinate low-spin d^7 complex, $[Co((C_6H_5)_2PCH_2CH_2P(C_6H_5)_2)_2Cl][SnCl_3]$, has also been found in both trigonal-bipyramidal and square-pyramidal forms: J. K. Stalick, P. W. R. Corfield, and D. W. Meek, *J. Amer. Chem. Soc.*, **94**, 6194 (1972). (d) E. L. Muetterties and R. A. Schunn, *Quart. Rev., Chem. Soc.*, **20**, 245 (1966). (e) J. A. Ibers, *Annu. Rev. Phys. Chem.*, **16**, 380 (1965). (f) J. S. Wood, *Progr. Inorg. Chem.*, **16**, 227 (1972).

(3) K. N. Raymond, P. W. R. Corfield, and J. A. Ibers, *Inorg. Chem.*, **7**, 1362 (1968).

(4) A. Terzis, K. N. Raymond, and T. G. Spiro, *Inorg. Chem.*, **9**, 2415 (1970).

(5) H. Schlaefer and O. Kling, *Z. Anorg. Allg. Chem.*, **302**, 1 (1959).

prepared using the method described by Raymond and Basolo.[6] Large, well-formed red crystals were obtained at −5°. Infrared spectra of the solids were recorded on a Perkin-Elmer 421 grating infrared spectrometer as Nujol mulls. Infrared cyanide stretching frequencies were found at 2142 (w), 2135 (m), 2125 (s), 2115 (s), 2090 (sh), and 2080 (w) cm^{-1}.

Crystal Examination. All crystals of $[Cr(tn)_3][Ni(CN)_5]\cdot 2H_2O$ and of $[Cr(NH_3)_6][Ni(CN)_5]\cdot 2H_2O$ chosen for X-ray studies exhibited sharp extinction under the polarizing microscope and were sealed in thin-walled glass capillaries to avoid loss of water. The lattice constants for each crystal were obtained by a least-squares refinement of the diffractometer setting angles of nine carefully centered reflections. The pertinent unit cell data for each crystal are given in Table I.

Data Collection. All data for both compounds were collected on an automated Picker four-circle diffractometer[7] using graphite monochromatized Mo Kᾱ radiation (λ 0.71069 Å). Crystals were not mounted along symmetry axes in order to minimize multiple diffraction effects.[8] Intensity data were collected by the θ–2θ scan technique as described previously.[9,10] The details for each data set are summarized in Table II.

$[Cr(tn)_3][Ni(CN)_5]\cdot 2H_2O$. Two data sets were collected at different temperatures. During the collection of the room-temperature data set (23°), the crystal decomposed in the X-ray beam to 14% of the original intensity. To compensate for the decomposition, a correction factor was calculated and applied to obtain the values of the intensity and standard deviation that would have been measured at the beginning of data collection. This data set was used for solution of the structure. A second data set was collected at −80 (2)°, a temperature at which the crystal was indefinitely stable to X-rays. A cold nitrogen flow system (Enraf–Nonius) was used to achieve a temperature of −80 (2)°. The variation of the intensities of three standards measured every 100 reflections was 7% and random during data collection. The low-temperature data were used in the final refinement of the structure to obtain the parameters and results reported here. There is little difference between the results obtained by the two data sets.

$[Cr(NH_3)_6][Ni(CN)_5]\cdot 2H_2O$. Data were collected at −10 (2)° using a nitrogen flow system to avoid decomposition of the crystal in the X-ray beam. Intensity standards were measured every 60 reflections. The standard deviation in intensities of the standards was 1%, indicating the dramatic increase in stability of the crystal at the lower temperature.

Data Reduction. The data sets for both compounds were extensively checked for errors and reduced to values of F^2 after correcting for Lorentz and polarization effects. A value of 0.04 was assigned to p in the calculations for both data sets.[9]

$[Cr(tn)_3][Ni(CN)_5]\cdot 2H_2O$. The absorption coefficient of $[Cr(tn)_3][Ni(CN)_5]\cdot 2H_2O$ for Mo Kα radiation is 14.2 cm^{-1}. For the first crystal, the transmission factors ranged from a minimum of 0.70 to a maximum of 0.77 and an absorption correction was applied using numerical integration.[11] An absorption correction was not applied to the low-temperature data set, since the transmission factors ranged from 0.73 to 0.78 for the data crystal. Of the 3299 observed reflections in the low-temperature data set, 2356 gave $F^2 > \sigma(F^2)$ and 1670 reflections gave $F^2 > 3\sigma(F^2)$.

$[Cr(NH_3)_6][Ni(CN)_5]\cdot 2H_2O$. Data were reduced as described above. An absorption correction was not applied. For a linear absorption correction of 21.4 cm^{-1} for Mo Kα radiation, the transmission factors ranged from a minimum of 0.56 to a maximum of 0.62. A total of 1253 reflections were observed, of which 1090 gave $F^2 > \sigma(F^2)$ and 942 gave $F^2 > 3\sigma(F^2)$.

Table I. Crystal Data

	$[Cr(tn)_3][Ni(CN)_5]\cdot 2H_2O$		$[Cr(NH_3)_6][Ni(CN)_5]\cdot 2H_2O$
Temp, °C	23°	−80°	−10°
Extinctions	$0kl$, $k \neq 2n$ $h0l$, $l \neq 2n$ $hk0$, $k \neq 2n$		$0kl$, $l \neq 2n$ $h0l$, $l \neq 2n$ $hk0$, $h \neq 2n$
Laue symmetry	*mmm*		*mmm*
Space group	*Pbca*		*Pcca*
a, Å	23.497 (6)	23.442 (7)	23.102 (10)
b, Å	13.306 (4)	13.239 (4)	11.529 (3)
c, Å	14.402 (4)	14.352 (6)	11.735 (4)
z	8	8	8
ρ_{calcd}, g/cm^3	1.47	1.49	1.61
ρ_{obsd}, g/cm^3	1.48		1.60
Flotation solution	Methylene chloride and toluene		Methylene bromide and toluene

Solution and Refinement of Structure. The positions of chromium and nickel atoms in both structures were located from Fourier syntheses in which normalized structure factors were substituted for unphased coefficients. Structure factors for all reflections were normalized[11] according to

$$E_{hkl} = F_{hkl}/\epsilon\left[\sum_{j=1}^{N} f_j^2{}_{hkl}\right]$$

F_{hkl} is observed structure factor which has been corrected for thermal motion. The factor ϵ adjusts for the degeneracy of F_{hkl} for reflections at symmetry locations in reciprocal space, and N is the number of atoms in the unit cell. The atomic scattering factor for the jth atom is f_j, scattering factors for neutral Cr, Ni, C, N, and O were those tabulated by Cromer and Mann.[12] The scattering factors of Stewart, *et al.*, were used for hydrogen.[13] The anomalous dispersion terms of f' and f'' for nickel and chromium were those of Cromer.[14] Phases were determined by reiterative application of Sayre's equation.[11,15] The initial sign set consisted of seven reflections of which three were needed to fix the origin. In the iterative process, newly calculated phases whose probabilities were greater than 95% were used in the next cycle to determine phases of the remaining reflections. Of the 16 possible solutions, the correctly phased solution was considered to have the highest consistency index and to require the least number of cycles to determine all phases. The consistency index is given by

$$C = \frac{\langle |E_{\mathbf{h}_1} \sum_{\mathbf{h}_2} E_{\mathbf{h}_1-\mathbf{h}_2} E_{\mathbf{h}_2}| \rangle}{\langle |E_{\mathbf{h}_1}| \sum_{\mathbf{h}_2} |E_{\mathbf{h}_1-\mathbf{h}_2}||E_{\mathbf{h}_2}| \rangle}$$

$[Cr(tn)_3][Ni(CN)_5]\cdot 2H_2O$. The structure was partially solved by direct methods. Phases for 110 reflections were determined by reiterative application of Sayre's equation. A Fourier synthesis was computed using the solution which had the highest consistency index of 0.997 and four cycles of reiteration to determine all phases. The highest peaks were assigned to chromium and nickel and three cyanide groups were also located.

$[Cr(NH_3)_6][Ni(CN)_5]\cdot 2H_2O$. An initial attempt to locate the metal atom positions from a three-dimensional unsharpened Patterson map gave four distinct but equally good solutions. The packing of the heavy atoms is that of a NaCl lattice array, which generates very severe pseudosymmetry. To break the ambiguity, direct methods were again employed. Structure factors for all reflections were normalized and phases for 207 reflections were determined by reiterative application of Sayre's equation. A Fourier synthesis was computed using the phasing model which had the highest consistency index (0.955) and the least number of cycles (4). The positions

(6) K. N. Raymond and F. Basolo, *Inorg. Chem.*, 5, 949 (1966).

(7) The diffractometer is automated by a PDP 8/I computer with 4K memory. Except for minor modifications, the controlling programs are those of Busing and Levy as modified by the Picker Corp.

(8) W. H. Zachariasen, *Acta Crystallogr.*, 18, 705 (1965).

(9) E. N. Duesler and K. N. Raymond, *Inorg. Chem.*, 10, 1468 (1971).

(10) The X-ray tube takeoff angle of 2.0° and pulse height analyzer were set to admit 95% of the Mo Kα radiation. All crystals were centered 30 cm from the counter aperture (7 mm × 7 mm). The scan was initiated SW/2° below $K\alpha_1$ and ended SW/2° above $K\alpha_2$. Backgrounds were counted at each end of the scan of width SW. Copper foil attenuators were automatically inserted if the intensity of the diffracted beam exceeded 10,000 counts/sec. Three reflections for each data set were measured periodically to monitor the stability of the crystals.

(11) In addition to various local programs for the CDC 6400 computer, local modifications of the following programs were employed: Hamilton's GONO absorption program, Dewar's FAME structure factor normalization program, Long's REL phase determination program, Zalkin's FORDAP Fourier program, the Doeden–Ibers group least-squares program NUCLS (based on the Busing–Levy ORFLS), the Busing–Levy program ORFFE, and Johnson's thermal ellipsoid program ORTEP.

(12) D. T. Cromer and J. B. Mann, *Acta Crystallogr., Sect. A*, 24, 321 (1968).

(13) R. F. Stewart, E. R. Davidson, and W. T. Simpson, *J. Chem. Phys.*, 42, 3175 (1965).

(14) D. T. Cromer, *J. Chem. Phys.*, 18, 17 (1965).

(15) D. Sayre, *Acta Crystallogr.*, 5, 60 (1952).

Table II. Data Collection

	$[Cr(tn)_3][Ni(CN)_5]\cdot 2H_2O$		$[Cr(NH_3)_6][Ni(CN)_5]\cdot 2H_2O$
λ, Å	0.71069	0.71069	0.71069
Temp, °C	23	−80 (2)	−10 (2)
Crystal size, mm	0.355 × 0.210 × 0.265	0.223 × 0.170 × 0.182	0.435 × 0.219 × 0.270
Initial ω width at half-height, deg	0.22	0.11–0.135	0.10
Final ω width at half-height, deg	0.30	0.11–0.135	0.10
Scan width, deg	1.10	1.80	1.2
Scan rate, deg/min	1	2	2
Background count, sec	10	4	4
Maximum bragg 2θ, deg	50	45	45
Periodicity of standards	60	100	60

Table IV. Positional and Thermal Parameters for $[Cr(tn)_3][Ni(CN)_5]\cdot 2H_2O$ at −80°

Atom	10^5x	10^5y	10^5z	$10^5\beta_{11}$[a]	$10^5\beta_{22}$	$10^5\beta_{33}$	$10^5\beta_{12}$	$10^5\beta_{13}$	$10^5\beta_{23}$
Ni	38032 (5)[b]	08370 (9)	18506 (8)	64 (2)	293 (8)	216 (6)	−1 (5)	6 (4)	26 (6)
NiC_1	39209 (38)	−02288 (73)	07459 (62)	81 (23)	356 (69)	202 (50)	−13 (31)	27 (25)	85 (53)
NiC_2	44057 (44)	17212 (83)	15194 (67)	104 (23)	420 (84)	262 (58)	67 (37)	−10 (30)	0 (7)
NiC_3	32664 (43)	16994 (79)	13326 (71)	101 (23)	242 (77)	354 (63)	−47 (34)	38 (30)	−97 (59)
NiC_4	31916 (39)	02393 (80)	25052 (62)	52 (20)	358 (86)	179 (56)	38 (33)	−68 (26)	75 (52)
NiC_5	43193 (40)	02665 (84)	26926 (70)	66 (21)	517 (102)	141 (51)	−51 (36)	48 (28)	−52 (58)
NiN_1	39915 (33)	−07704 (65)	01542 (53)	187 (21)	412 (65)	170 (42)	34 (31)	49 (25)	−60 (48)
NiN_2	47904 (36)	22165 (64)	13435 (63)	126 (20)	394 (75)	537 (61)	−73 (30)	69 (29)	−18 (54)
NiN_3	29087 (40)	22375 (67)	10595 (63)	169 (22)	491 (79)	451 (60)	54 (34)	16 (30)	62 (56)
NiN_4	28243 (31)	−01250 (66)	28811 (54)	51 (16)	584 (70)	295 (51)	−13 (28)	−30 (22)	223 (48)
NiN_5	46525 (32)	−00987 (67)	31717 (57)	85 (17)	692 (76)	267 (48)	22 (31)	−42 (25)	110 (55)
Cr	37415 (6)	51605 (10)	23615 (9)	55 (2)	216 (8)	172 (8)	10 (6)	0 (4)	9 (7)
CrN_1	42068 (29)	64798 (58)	20951 (45)	69 (16)	295 (54)	155 (41)	12 (25)	−4 (19)	−63 (40)
CrN_2	32624 (28)	59138 (58)	33839 (45)	70 (15)	261 (52)	133 (41)	−16 (25)	6 (19)	27 (39)
CrN_3	41993 (29)	43664 (56)	13525 (48)	76 (16)	302 (58)	169 (40)	11 (24)	23 (20)	−69 (40)
CrN_4	31197 (30)	55017 (54)	13581 (50)	71 (15)	262 (55)	224 (43)	34 (23)	−7 (21)	6 (39)
CrN_5	43728 (29)	47769 (57)	33414 (47)	58 (15)	305 (57)	172 (41)	18 (25)	3 (20)	80 (41)
CrN_6	32898 (30)	38546 (54)	27328 (51)	82 (16)	206 (53)	250 (41)	3 (24)	−1 (21)	71 (39)
CrC_1	39247 (38)	74854 (80)	21966 (68)	116 (22)	209 (60)	379 (58)	7 (32)	−33 (28)	58 (51)
CrC_{1-2}	36570 (39)	76425 (67)	31319 (66)	151 (25)	138 (58)	348 (54)	30 (30)	45 (32)	76 (53)
CrC_2	31291 (43)	70137 (74)	32998 (66)	153 (23)	342 (71)	242 (62)	113 (35)	25 (32)	−64 (51)
CrC_3	42020 (36)	46768 (76)	03578 (60)	70 (18)	472 (73)	106 (46)	−11 (33)	24 (24)	4 (49)
CrC_{3-4}	36154 (36)	48188 (81)	−00328 (59)	116 (24)	647 (87)	92 (44)	24 (36)	17 (25)	−15 (54)
CrC_4	32929 (40)	57017 (79)	03648 (63)	119 (22)	455 (82)	200 (56)	20 (35)	19 (27)	140 (58)
CrC_5	44550 (48)	36867 (91)	35324 (79)	124 (25)	674 (99)	582 (76)	46 (41)	−119 (36)	246 (75)
CrC_{5-6}	39624 (50)	31056 (92)	39094 (79)	191 (31)	702 (98)	434 (74)	−67 (44)	−72 (38)	190 (71)
CrC_6	34013 (54)	34485 (106)	36623 (89)	195 (32)	944 (126)	784 (94)	−146 (52)	−63 (44)	72 (94)
O_1	23399 (26)	39975 (52)	05157 (48)	127 (15)	478 (54)	568 (47)	−21 (26)	−7 (21)	−36 (43)
O_2	04705 (26)	22461 (44)	02363 (41)	133 (15)	341 (50)	273 (37)	49 (21)	8 (19)	96 (36)

[a] The form of the thermal ellipsoid is $\exp[-(\beta_{11}h^2 + \beta_{22}k^2 + \beta_{33}l^2 + 2\beta_{12}hk + 2\beta_{13}hl + 2\beta_{23}kl)]$. [b] Numbers in parentheses, here and in succeeding tables, are the estimated standard deviations in the least significant digits.

of the highest peaks were assigned to chromium and nickel. This corresponded to one of the four possible Patterson solutions.

Refinement. The remaining atoms for both compounds were located by standard least-squares and Fourier techniques.[16]

$[Cr(tn)_3][Ni(CN)_5]\cdot 2H_2O$. Using the low-temperature data set, all nonhydrogen atoms were refined anisotropically with the same model used for the room-temperature set.[16] For the final calculation, 1671 reflections with $F^2 > 3\sigma(F^2)$ gave R_1 and R_2 values of 5.1 and 5.4%. The error in an observation of unit weight was 1.53. The ten highest peaks in the final difference Fourier ranged from 0.20 to 0.32 e/Å^3 and all were ripples near the chromium and nickel atom positions. The final observed and calculated structure factors for the low-temperature structure of $[Cr(tn)_3][Ni(CN)_5]\cdot 2H_2O$ are given in Table III.[17] The final low-temperature positional and thermal parameters are given in Table IV for the nonhydrogen atoms and in Table V[17] for the hydrogen atoms.

$[Cr(NH_3)_6][Ni(CN)_5]\cdot 2H_2O$. A difference Fourier was calculated in which all reflections with $(\sin\theta)/\lambda > 0.4$ were rejected. Most amine hydrogen atoms were revealed. In subsequent computations, the ligand hydrogens were refined as part of six rigid amine groups. The N–H bonds were fixed at 1.0 Å and the Cr–N–H angle was fixed at 109°. Threefold symmetry was imposed on the NH_3 group with the symmetry axis coincident with the Cr–N bond. This leaves one group orientation angle to be refined in order to obtain the correct positional parameters of the hydrogens. An isotropic temperature factor of 3.0 Å^2 was assigned to each hydrogen atom. The hydrogens corresponding to the waters of crystallization could not be found.

The final anisotropic refinement of nonhydrogen atoms was based on F and included 1090 intensities with $F^2 > \sigma(F^2)$. The final error in an observation of unit weight is 1.69. Since the value of this quantity did not depend uniformly upon the magnitude of the intensities, the weighting scheme was not adjusted. The final values of R_1 and R_2 are 4.07 and 4.68%, respectively. The electron density in the final difference Fourier varied from 0.262 to 0.340 e/Å^3 for the first ten peaks. The final observed and calculated structure factors for the low-temperature structure of $[Cr(NH_3)_6][Ni(CN)_5]\cdot 2H_2O$ are given in Table VI.[17] The final low-temperature positional

(16) The function $w(|F_o| - |F_c|)^2$ was minimized in the least-squares refinements in which $|F_o|$ and $|F_c|$ are the observed and calculated structure factor amplitudes, respectively, and w is the weighting factor given by $4F_o^2/\sigma^2(F_o^2)$. In a final difference Fourier for the room-temperature data set of $[Cr(tn)_3][Ni(CN)_5]\cdot 2H_2O$, all reflections with $(\sin\theta)/\lambda \geq 0.4$ were rejected in an unsuccessful attempt to locate the remaining hydrogen atoms. The positions of the hydrogens on the 1,3-propanediamine ligands were calculated from the C and N atom positions.[11] The C–H or N–H bond length was assumed to be 1.0 Å and the H–C–H or H–N–H angle assumed to be 109°. All hydrogens were assigned a thermal factor of 4.0 Å^2 and their scattering amplitudes were added as fixed contributions to the calculated structure factors in subsequent refinements. An anisotropic refinement of all nonhydrogen atoms using $F^2 \geq 3\sigma(F^2)$ lowered R_1 and R_2 to 6.2 and 6.9%, where $R_1 = \Sigma\,||F_o| - |F_c||/\Sigma\,|F_o|$ and $R_2 = [\Sigma w(|F_o| - |F_c|)^2/\Sigma w|F_o|^2]^{1/2}$. The standard deviations of the 262 parameters were significantly lower when the 850 reflections with $1\sigma \geq F^2 \geq 3\sigma$ were included. The error in an observation of unit weight defined as $[\Sigma w(|F_o| - |F_c|)^2/(N_o - N_v)]^{1/2}$ was 2.16 (where N_o and N_v are the number of observations and variables) and the values of R_1 and R_2 increased to 10.7 and 8.3%.

(17) See paragraph at end of paper regarding supplementary material.

Table VII. Positional and Thermal Parameters for $[Cr(NH_3)_6][Ni(CN)_5]\cdot 2H_2O$ at −10°

Atom	10^5x	10^5y	10^5z	$10^5\beta_{11}$[a]	$10^5\beta_{22}$	$10^5\beta_{33}$	$10^5\beta_{12}$	$10^5\beta_{13}$	$10^5\beta_{23}$
Ni	12253 (4)	26489 (6)	05025 (7)	151 (4)	388 (7)	382 (7)	17 (4)	−4 (4)	−26 (5)
NiC_1	19140 (38)	20458 (57)	15105 (56)	121 (29)	521 (58)	332 (57)	−10 (35)	−30 (35)	−41 (47)
NiC_2	15993 (37)	38495 (59)	−02791 (59)	156 (28)	454 (60)	540 (63)	95 (58)	−42 (35)	−111 (50)
NiC_3	13058 (33)	17302 (55)	−08050 (55)	145 (27)	428 (55)	417 (53)	−44 (33)	20 (34)	114 (46)
NiC_4	06424 (37)	16136 (60)	09268 (56)	88 (28)	513 (60)	423 (56)	−4 (37)	3 (34)	−40 (47)
NiC_5	09178 (36)	37598 (52)	15300 (56)	159 (26)	373 (52)	447 (56)	−9 (34)	−28 (34)	45 (45)
NiN_1	22899 (32)	17747 (56)	20617 (48)	173 (26)	959 (65)	422 (53)	22 (34)	−7 (31)	−126 (48)
NiN_2	18076 (29)	46026 (49)	−07731 (52)	184 (22)	510 (52)	854 (59)	10 (33)	−12 (31)	59 (45)
NiN_3	13394 (30)	11710 (46)	−16044 (46)	265 (24)	510 (48)	417 (48)	−15 (30)	76 (29)	−36 (39)
NiN_4	02916 (30)	09394 (56)	11170 (51)	142 (24)	759 (60)	674 (58)	−25 (32)	23 (30)	−60 (50)
NiN_5	07309 (30)	44479 (49)	21172 (46)	260 (23)	564 (47)	599 (55)	48 (30)	2 (30)	−162 (44)
Cr	12360 (5)	−22596 (8)	02516 (8)	139 (5)	327 (9)	314 (8)	−12 (4)	8 (5)	−8 (6)
CrN_1	05233 (24)	−17042 (43)	11861 (43)	105 (18)	490 (44)	491 (45)	18 (25)	98 (26)	−24 (37)
CrN_2	19928 (25)	−28221 (40)	−05479 (41)	105 (19)	482 (45)	453 (44)	19 (24)	51 (24)	−2 (36)
CrN_3	07634 (25)	−36779 (40)	−03048 (43)	138 (18)	455 (43)	487 (46)	−39 (25)	20 (26)	−74 (36)
CrN_4	16661 (24)	07917 (39)	08038 (40)	123 (17)	356 (41)	433 (41)	−26 (25)	−20 (24)	−46 (34)
CrN_5	15047 (27)	−32201 (42)	16625 (40)	165 (18)	437 (45)	382 (41)	−10 (26)	31 (24)	12 (35)
CrN_6	09819 (24)	−13732 (42)	−12167 (41)	93 (16)	558 (44)	372 (41)	−22 (26)	−11 (25)	15 (35)
O_1	47372 (22)	37395 (40)	36664 (42)	214 (42)	732 (44)	931 (50)	55 (24)	11 (26)	76 (39)
O_2	25000 (0)	50000 (0)	18576 (65)	407 (31)	1625 (102)	729 (73)	96 (48)	0 (0)	0 (0)
O_3	25000 (0)	00000 (0)	40283 (49)	165 (21)	779 (61)	440 (54)	−64 (31)	0 (0)	0 (0)

[a] The form of the thermal ellipsoid is $\exp[-(\beta_{11}h^2 + \beta_{22}k^2 + \beta_{33}l^2 + 2\beta_{12}hk + 2\beta_{13}hl + 2\beta_{23}kl)]$.

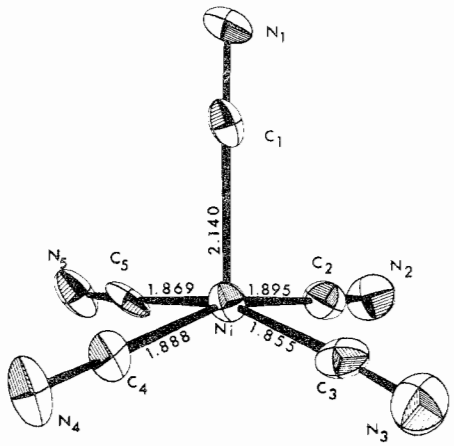

Figure 1. A perspective drawing of the square-pyramidal $[Ni(CN)_5]^{3-}$ ion in $[Cr(tn)_3][Ni(CN)_5]\cdot 2H_2O$ at −80°. The shapes of the atoms in this and following drawings represent 50% probability contours of the thermal motion.

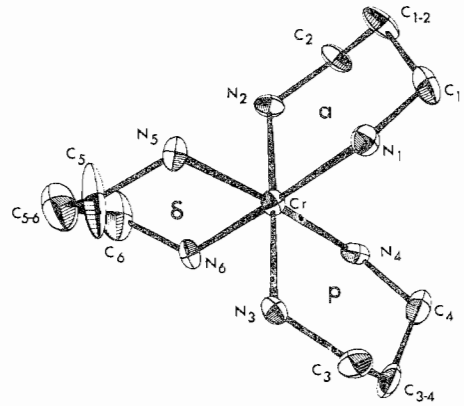

Figure 2. A perspective view down the pseudo-threefold axis of the $[Cr(tn)_3]^{3+}$ cation. Starting with the upper right ring and moving clockwise, the rings are referred to as ring 1 (a conformer), ring 2 (p conformer), and ring 3 (δ conformer).

and thermal parameters are given in Table VII for the nonhydrogen atoms and in Table VIII[17] for the hydrogen atoms.

Description of the Structures

$[Cr(tn)_3][Ni(CN)_5]\cdot 2H_2O$. The structure of tris(1,3-propanediamine)chromium pentacyanonickelate dihydrate consists of discrete $[Cr(tn)_3]^{3+}$ and $[Ni(CN)_5]^{3-}$ ions linked together in a network of hydrogen bonds. Each ion is surrounded by an elongated octahedron of counterions. For nickel at the center of the octahedron, the interatomic distances to chromium atoms at opposite vertices are 5.77 and 7.55 Å, 5.93 and 6.08 Å, and 6.58 and 8.02 Å. The packing of the ions in the crystal approximates a face-centered cubic lattice. An idealized supercell can be constructed for which the origin is $^3/_8, 0, ^1/_4$ in the true cell coordinates and the *a* cell edge is half that of the old. The deviation from a sodium chloride structure is greater than that found in the $[Cr(en)_3]^{3+}$ salt[3] and much greater than that in the $[Cr(NH_3)_6]^{3+}$ salt.

A perspective drawing of the $[Ni(CN)_5]^{3-}$ complex is shown in Figure 1. The geometry of the anion is a regular square pyramid, with an apical bond length much longer than the basal bond lengths. The apical Ni–C bond is 2.140 (10) Å. Averaged angles for the trans basal C–Ni–C angles and for the C_{apical}–Ni–C_{basal} angles are 161.5 (2) and 99.2 (1.1)°, respectively. The nickel atom lies 0.301 Å above the basal plane of carbons and 0.477 Å above the nitrogen plane. There is no coordination to nickel below the basal plane; the nearest atom is oxygen O_1, at a distance of 4.10 Å. In Table IX the bond lengths, angles, and standard deviations estimated from the variance–covariance matrix for this anion are compared to values obtained for the anions of the $[Cr(en)_3]^{3+}$ (C_4 form)[3] and the $[Cr(NH_3)_6]^{3+}$ salts. The root-mean-square amplitudes of vibration for the thermal ellipsoids of each atom are given in Table X. The equations for best weighted least-squares plane through various combinations of atoms are in Table XI.[17]

In Figure 2 the cation is shown as viewed down the coordination pseudo-threefold axis. The nitrogen atoms of the three 1,3-propanediamine rings form a slightly distorted octahedron around the chromium. Two of the six-membered chelate rings have the expected stable chair conformation. The two chair rings are related by a molecular twofold axis which bisects the remaining ring and is perpendicular to the coordination pseudo-threefold axis. *The third ring has a skew-boat or twist conformation analogous to the twist form of the flexible conformation of cyclohexane.* Much greater thermal motion is observed in the carbon atoms of the twist ring relative to

Table IX. Comparison of Bond Distances (Å) and Bond Angles (deg) in Three Square-Pyramidal $[Ni(CN)_5]^{3-}$ Structures

Bond	$[Cr(en)_3]^{3+}$ [a]	$[Cr(tn)_3]^{3+}$	$[Cr(NH_3)_6]^{3+}$
Distances			
$Ni-C_1$	2.168 (14)	2.140 (10)	2.101 (9)
$Ni-C_2$	1.867 (14)	1.895 (11)	1.872 (8)
$Ni-C_3$	1.872 (12)	1.855 (12)	1.874 (7)
$Ni-C_4$	1.839 (13)	1.888 (10)	1.867 (9)
$Ni-C_5$	1.869 (13)	1.869 (11)	1.897 (7)

	No.	$[Cr(en)_3]^{3+}$	$[Cr(tn)_3]^{3+}$	$[Cr(NH_3)_6]^{3+}$
Weighted Average Bond Distances and Bond Angles				
Bond type: Basal Ni–C	4	1.862 (6)	1.877 (9)	1.877 (7)
Bond type: Basal Ni–N	4	3.017 (5)	3.021 (6)	3.020 (5)
Bond type: C–N	5	1.153 (5)	1.141 (8)	1.140 (4)
Angle: C_{apical}–Ni–C_{basal}	4	100.2 (15)	99.2 (11)	100.1 (6)
Angle: Trans C_{basal}–Ni–C_{basal}	2	159.5 (2)	161.5 (3)	159.70 (2)

[a] C_{4v} form.

Table X. Root-Mean-Square Amplitude (Å)[a] for $[Cr(tn)_3][Ni(CN)_5]\cdot 2H_2O$

Atom	Min	Intermed	Max	Atom	Min	Intermed	Max
Ni	0.133 (2)	0.147 (3)	0.166 (2)	Cr	0.122 (3)	0.133 (3)	0.142 (3)
NiC_1	0.117 (23)	0.160 (19)	0.190 (18)	CrN_1	0.115 (19)	0.137 (16)	0.172 (15)
NiC_2	0.147 (22)	0.167 (19)	0.211 (19)	CrN_2	0.113 (19)	0.138 (16)	0.157 (16)
NiC_3	0.124 (25)	0.159 (20)	0.214 (18)	CrN_3	0.110 (19)	0.152 (15)	0.174 (15)
NiC_4	0.044 (56)	0.168 (19)	0.187 (20)	CrN_4	0.125 (17)	0.154 (15)	0.165 (15)
NiC_5	0.090 (29)	0.146 (21)	0.223 (21)	CrN_5	0.115 (19)	0.126 (17)	0.179 (15)
NiN_1	0.117 (20)	0.194 (15)	0.234 (13)	CrN_6	0.120 (19)	0.151 (14)	0.173 (14)
NiN_2	0.148 (18)	0.204 (16)	0.251 (14)	CrC_1	0.130 (21)	0.174 (18)	0.208 (15)
NiN_3	0.189 (17)	0.211 (15)	0.240 (15)	CrC_{1-2}	0.100 (26)	0.177 (18)	0.221 (17)
NiN_4	0.109 (20)	0.139 (18)	0.256 (13)	CrC_2	0.114 (25)	0.173 (19)	0.235 (16)
NiN_5	0.134 (18)	0.173 (16)	0.255 (14)	CrC_3	0.097 (25)	0.145 (18)	0.205 (16)
				CrC_{3-4}	0.096 (24)	0.180 (18)	0.241 (16)
O_1	0.184 (12)	0.208 (12)	0.245 (10)	CrC_4	0.118 (24)	0.179 (17)	0.220 (18)
O_2	0.138 (15)	0.179 (12)	0.212 (11)	CrC_5	0.124 (25)	0.232 (18)	0.293 (17)
				CrC_{5-6}	0.179 (21)	0.215 (19)	0.287 (17)
				CrC_6	0.108 (33)	0.225 (19)	0.397 (19)

[a] The directions of these principal axes of vibrations are displayed in the various figures.

those of the two other rings. Perspective views of all three rings are shown in Figure 3.

In the chelate rings, the average Cr–N bond distance is 2.096 (3) Å and the average N–Cr–N angle is 89.7 (3)°. The remaining internal bond angles and distances in the chair conformers differ considerably from the skew-boat geometry. The average Cr–N–C, N–C–C, and C–C–C bond angles are 120.7 (4), 112.4 (5), and 114.4 (2)° in the chair rings. In the skew-boat conformer, the respective angles are 116.6 (2), 119.2 (12), and 117.2 (10)°. The average N–C and C–C distances are 1.495 (4) and 1.502 (3) Å in the chair conformers and 1.472 (10) and 1.462 (27) Å in the skew-boat conformer. Some difference may be attributed to error introduced by the high correlation of the positional parameters with the large thermal motion present in the rings, particularly in the skew-boat conformer. In Table XII the bond lengths, angles, and standard deviations are given for the cation.

The main features of the hydrogen-bonding network are illustrated in the stereoscopic packing diagram shown in Figure 4. The significant hydrogen bonds formed among the amine protons, cyanide nitrogens, and oxygens from the waters of crystallization are listed in Table XIII. The hydrogen-bonding network can be best described by the role of the waters of crystallization. The first water molecule, designated O_1, is the link between anions related by the *b* glide plane. Linear chains are formed along the *b* axis by O_1 bonding to the apical cyanide nitrogen NiN_1 and the basal nitrogen atom NiN_3 of the glide-related anion, and O_1 is also hydrogen bonded to a proton on CrN_4. Through the second water molecule, O_2, centrosymmetrically related chains of glide-related anions are linked together. The hydrogen bonds of O_2 are formed with the apical NiN_1, and the basal NiN_2 of the centrosymmetrically related anion and also with a neighboring cation to CrN_1.

$[Cr(NH_3)_6][Ni(CN)_5]\cdot 2H_2O$. The structure of hexaammine-chromium pentacyanonickelate(II) dihydrate consists of discrete $[Cr(NH_3)_6]^{3+}$ and $[Ni(CN)_5]^{3-}$ ions which are all linked by hydrogen bonds. Each cation and anion is surrounded by six oppositely charged ions, closely approximating a face-centered cubic lattice array. With nickel at the center of an octahedron, the interatomic distances to the chromium atoms in opposite corners are 5.67 and 5.77 Å, 5.88 and 5.89 Å, and 5.59 and 6.18 Å.

The origin of the supercell is $^1/_8$, $^1/_4$, 0 in the true cell coordinates and the *a* cell edge of the supercell is half that of the old. The Ni–Cr distance in the real cell deviates no more than 0.43 Å from the Ni–Cr distance of 5.75 Å for an idealized cubic cell.

A perspective view of the $[Ni(CN)_5]^{3-}$ anion is shown in Figure 5. The apical Ni–C distance is 2.101 (9) Å and the average basal Ni–C distance is 1.877 (7) Å. Important angles include the average trans basal C–Ni–C angle of 159.7 (2)° and the average C_{apical}–Ni–C_{basal} angle of 100.1 (6)°. The nickel atom lies above the basal plane, 0.330 Å from the plane of four carbons and 0.564 Å from the plane of four nitrogens. The atom with the closest approach to the nickel ion from below the basal plane is O_1, at a distance of 3.34 Å, too distant to be considered part of the coordination sphere. The root-mean-square amplitudes of vibration for the thermal

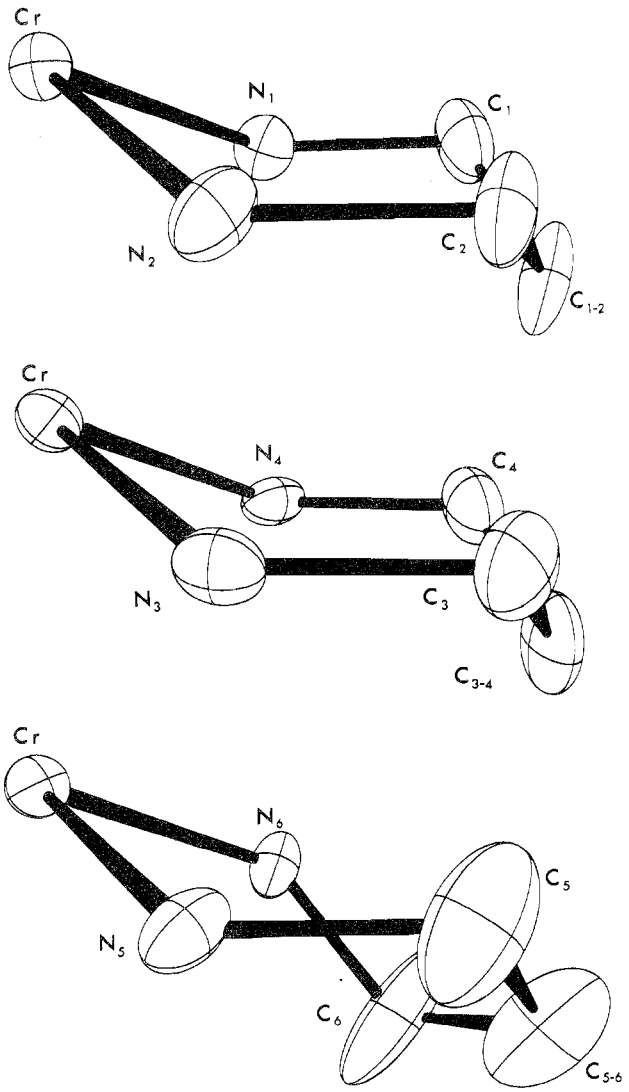

Figure 3. Perspective drawings of the individual 1,3-propanediamine rings. All are drawn on the same scale for a direct comparison of the ring features, particularly the large thermal motion in the third (skew-boat) ring.

ellipsoids of each atom are given in Table XIV. The equations for best weighted least-squares planes through various combinations of atoms are in Table XV.[17]

In the octahedral cation (Figure 6)[17] the average Cr-N bond distance is 2.080 (4) Å, slightly longer than the Cr-N distances given for $[Cr(NH_3)_6][CuCl_5]$, 2.0644 (25) Å,[18] and $[Cr(NH_3)_6][CuBr_5]$, 2.0592 (57) Å.[19] Bond lengths, angles, standard deviations and root-mean-square amplitudes of vibration along the principal axes of the thermal ellipsoids are given in Tables XVI[17] and XIV for each atom.

The main features of the hydrogen-bonding network are illustrated in the stereoscopic packing diagram of Figure 7. The significant hydrogen bonds formed among the NH_3 and CN groups and waters of crystallization are listed in Table XVII. The hydrogen-bonding network can be best described by the role of the waters of crystallization. The first water molecule, O_1, lies in a general position and links twofold-related chains of glide-related anions. The linkage between the chains occurs through a water-water hydrogen bond.

(18) K. N. Raymond, D. W. Meek, and J. A. Ibers, *Inorg. Chem.*, 7, 1111 (1968).
(19) S. A. Goldfield and K. N. Raymond, *Inorg. Chem.*, 10, 2604 (1971).

Table XII. Bond Distances (Å) and Bond Angles (deg) for the $[Cr(tn)_3]^{3+}$ Cation

Atoms	Dist	Atoms	Dist	Atoms	Dist
$Cr-N_1$	2.094 (8)	N_1-C_1	1.494 (11)	C_1-C_{1-2}	1.496 (13)
$Cr-N_2$	2.100 (7)	N_2-C_2	1.494 (11)	C_2-C_{1-2}	1.511 (12)
$Cr-N_3$	2.087 (7)	N_3-C_3	1.486 (10)	C_3-C_{3-4}	1.497 (11)
$Cr-N_4$	2.098 (7)	N_4-C_4	1.506 (11)	C_4-C_{3-4}	1.504 (13)
$Cr-N_5$	2.104 (7)	N_5-C_5	1.482 (12)	C_5-C_{5-6}	1.489 (14)
$Cr-N_6$	2.096 (7)	N_6-C_6	1.462 (12)	C_6-C_{5-6}	1.436 (16)
Wtd av	2.096 (3)				

Atoms	Angles	Atoms	Angles
N_1-Cr-N_2	90.58 (28)	$C_1-C_{1-2}-C_2$	114.20 (83)
N_3-Cr-N_4	89.39 (27)	$C_3-C_{3-4}-C_4$	114.66 (80)
N_5-Cr-N_6	89.21 (29)	$C_5-C_{5-6}-C_6$	117.20 (98)
$Cr-N_1-C_1$	119.66 (53)	$N_1-C_1-C_{1-2}$	113.40 (77)
$Cr-N_2-C_2$	121.21 (56)	$N_2-C_2-C_{1-2}$	112.25 (75)
$Cr-N_3-C_3$	121.99 (56)	$N_3-C_3-C_{3-4}$	112.99 (69)
$Cr-N_4-C_4$	120.02 (54)	$N_4-C_4-C_{3-4}$	110.97 (78)
$Cr-N_5-C_5$	116.76 (60)	$N_5-C_5-C_{5-6}$	118.00 (97)
$Cr-N_6-C_6$	116.42 (67)	$N_6-C_6-C_{5-6}$	120.36 (1.08)
N_1-Cr-N_3	91.46 (27)	N_2-Cr-N_5	91.36 (27)
N_1-Cr-N_4	93.27 (28)	N_2-Cr-N_6	86.78 (28)
N_1-Cr-N_5	87.54 (28)	N_3-Cr-N_5	88.88 (28)
N_1-Cr-N_6	175.77 (28)	N_3-Cr-N_6	91.18 (29)
N_2-Cr-N_3	177.94 (29)	N_4-Cr-N_5	178.11 (29)
N_2-Cr-N_4	90.33 (29)	N_4-Cr-N_6	90.06 (28)

Weighted Average of Bond Angles

Angle type	No.	Chair conformers	No.	Skew boat
N-Cr-N	2	89.98 (60)	1	89.21
Cr-N-C	4	120.72 (40)	2	116.59 (17)
N-C-C	4	112.40 (53)	2	119.18 (1.18)
C-C-C	2	114.43 (23)	1	117.20

Dihedral Angles for Skew-Boat Ring

Plane 1 atoms	Plane 2 atoms	Angle, deg
N_5-Cr-N_6	$C_5-C_{5-6}-C_6$	28.5
$Cr-N_5-C_5$	$N_6-C_6-C_{5-6}$	82.7
$Cr-N_6-C_6$	$N_5-C_5-C_{5-6}$	75.3

Ring	Atoms	Conformn
1	$Cr-N_1-C_1-C_{1-2}-C_2-N_2$	Chair "a"
2	$Cr-N_3-C_3-C_{3-4}-C_4-N_4$	Chair "p"
3	$Cr-N_5-C_5-C_{5-6}-C_6-N_6$	Skew boat δ

Table XIII. Summary of Proposed A-H···B Hydrogen Bonds for $[Cr(tn)_3][Ni(CN)_5]\cdot 2H_2O$[a]

B	A	H	A-B, Å	H···B, Å	A-H···B, deg
NiN_1	CrN_2 (7)[b]	H_1	3.07	2.08	167.3
NiN_1	CrN_5 (7)	H_1	3.05	2.05	174.9
NiN_1	O_1[c] (6)		3.18		
NiN_1	O_2 (6)		2.92		
NiN_2	O_2 (2)		2.86		
NiN_3	O_1 (1)		2.80		
NiN_4	CrN_2 (6)	H_2	2.98	2.01	155.8
NiN_4	CrN_6 (6)	H_2	2.95	2.02	154.7
NiN_5	CrN_3 (3)	H_2	2.87	1.92	156.4
NiN_5	CrN_5 (3)	H_2	3.16	2.33	139.2
O_1	CrN_4 (1)	H_2	2.96	2.06	146.9
O_2	CrN_1 (6)	H_1	2.95	2.07	142.0
				Av	154.6

[a] Only A···B distances less than 3.1 Å for O···O distances or less than 3.2 Å for O···N or N···N distances are considered as significant hydrogen bonds. [b] These numbers correspond to the following transformations of the positions of the A atoms as given in Table IV: (1) x, y, z; (2) $1/2 + x, 1/2 - y, -z$; (3) $-x, 1/2 + y, 1/2 - z$; (4) $1/2 - x, -y, 1/2 + z$; (5) $-x, -y, -z$; (6) $1/2 - x, 1/2 + y, z$; (7) $x, 1/2 - y, 1/2 + z$; (8) $1/2 + x, y, 1/2 - z$. [c] The positions of the hydrogen atoms on the water molecules were not located.

Atom O_1 forms hydrogen bonds with the twofold-related O_1'. Each O_1 oxygen atom is also linked to the basal NiN_5 of the nearest anion and to CrN_3 and CrN_1 of the nearest

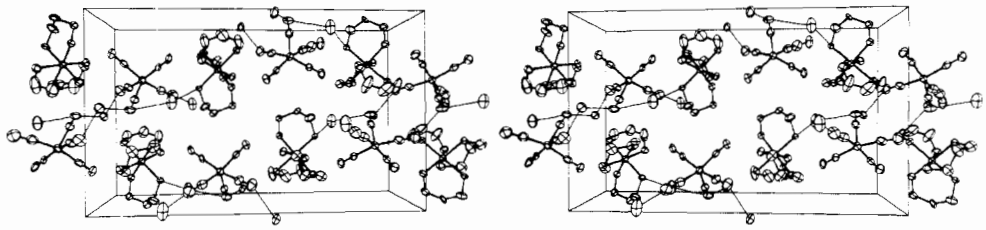

Figure 4. A stereoscopic packing diagram of the *xz* plane of $[Cr(tn)_3][Ni(CN)_5]\cdot 2H_2O$. The long axis is in the *x* direction. Only the water hydrogen bonds are illustrated.

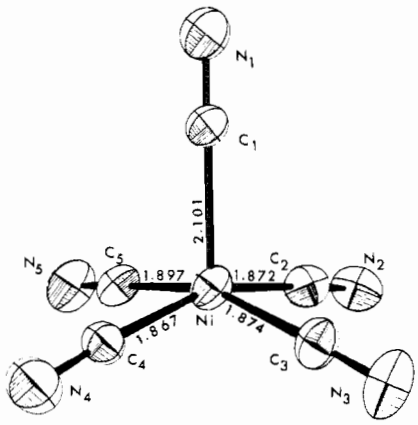

Figure 5. A perspective drawing of the square-pyramidal $[Ni(CN)_5]^{3-}$ ion in $[Cr(NH_3)_6][Ni(CN)_5]\cdot 2H_2O$ at $-10°$.

Table XIV. Root-Mean-Square Amplitudes of Vibration (Å) in $[Cr(NH_3)_6][Ni(CN)_5]\cdot 2H_2O$

Atom	Min	Intermed	Max
Ni	0.156 (2)	0.166 (2)	0.202 (3)
NiC_1	0.144 (16)	0.184 (18)	0.188 (12)
NiC_2	0.146 (16)	0.183 (14)	0.234 (15)
NiC_3	0.138 (14)	0.189 (13)	0.204 (17)
NiC_4	0.154 (24)	0.168 (11)	0.188 (11)
NiC_5	0.154 (11)	0.176 (12)	0.210 (16)
NiN_1	0.165 (11)	0.214 (16)	0.258 (9)
NiN_2	0.182 (10)	0.222 (13)	0.245 (8)
NiN_3	0.161 (11)	0.185 (9)	0.271 (11)
NiN_4	0.192 (17)	0.210 (10)	0.233 (10)
NiN_5	0.167 (10)	0.224 (9)	0.266 (12)
Cr	0.146 (2)	0.149 (2)	0.194 (4)
CrN_1	0.130 (16)	0.182 (8)	0.212 (10)
CrN_2	0.149 (14)	0.179 (8)	0.193 (11)
CrN_3	0.161 (10)	0.180 (12)	0.207 (11)
CrN_4	0.145 (11)	0.176 (9)	0.187 (12)
CrN_5	0.159 (10)	0.171 (9)	0.213 (12)
CrN_6	0.154 (14)	0.162 (11)	0.195 (8)
O_1	0.210 (8)	0.243 (9)	0.260 (8)
O_2	0.225 (11)	0.310 (12)	0.349 (12)
O_3	0.175 (11)	0.197 (14)	0.240 (10)

[a] The directions of these principal axes of vibration are displayed in the various figures.

cation. Since this twofold axis is parallel to *y*, the NiN_5-O_1-O_1'-NiN_5' group is easily discernible in the packing diagram of Figure 7 in the form of a "W." The second water molecule, on a twofold axis, is bonded only through the oxygen, O_2, to the hydrogens of the twofold-related NH_3 nitrogen, CrN_5. The twofold related cyanide nitrogen atoms, NiN_2, have the proper orientation to hydrogen bond to this water molecule but the twofold-related nitrogens are too distant (3.22 Å) from the oxygen to form strong hydrogen bonds. The hydrogen atoms of the remaining water of crystallization, O_3, apparently bond to two cyanides, NiN_1 and NiN_3, to form linear chains of *c*-glide-related anions. Since the O_3 oxygen atom lies on a twofold axis, there are four apparent hydrogen bonds between the water protons and the cyanide nitrogens. This is apparently due to a statistical disorder of the protons in the water of crystallization O_3. A third (and fourth) hydrogen bond is formed between O_3 and an NH_3 hydrogen of CrN_4.

Table XVII. Summary of Proposed A-H···B Hydrogen Bonds for $[Cr(NH_3)_6][Ni(CN)_5]\cdot 2H_2O$[a]

B	A	H	A-B Å	H···B Å	A-H···B deg
NiN_1	CrN_2 (8)[b]	H_3	3.13	2.14	166.8
NiN_1	CrN_4 (2)	H_2	3.05	2.18	143.4
NiN_1	O_3[c] (1, 2)[d]		3.12		
NiN_2	CrN_2 (1)	H_1	3.01	2.01	171.4
NiN_2	CrN_3 (1)	H_2	3.17	2.20	162.8
NiN_3	CrN_5 (8)	H_2	3.14	2.26	146.0
NiN_3	CrN_6 (1)	H_1	3.08	2.13	158.1
NiN_3	O_3 (7)		3.09		
NiN_4	CrN_1 (1)	H_3	3.10	2.35	130.7
NiN_4	CrN_6 (5)	H_2	2.99	1.98	179.4
NiN_5	CrN_3 (8)	H_2	3.15	2.20	162.8
NiN_5	O_1 (2)		2.98		
O_1	CrN_1 (3)	H_2	2.97	1.97	177.0
O_1	CrN_3 (3)	H_1	3.05	2.09	160.8
O_1	O_1 (4)		3.00		
O_2	CrN_5 (1, 2)[d]	H_3	3.09	2.18	150.6
O_3	CrN_4 (7, 8)[d]	H_1	2.98	1.98	175.4
				Av	160.4

[a] Only A···B distances less than 3.1 Å for O···O distances or less than 3.2 Å for O···N or N···N distances are considered as significant hydrogen bonds. [b] These numbers correspond to the following transformations of the positions of the A atoms as given in Table VII: (1) x, y, z; (2) $\frac{1}{2}-x, -y, z$; (3) $\frac{1}{2}+x, -y, \frac{1}{2}-z$; (4) $-x, y, \frac{1}{2}-z$; (5) $-x, -y, -z$; (6) $\frac{1}{2}+x, y, -z$; (7) $\frac{1}{2}-x, y, \frac{1}{2}+z$; (8) $x, -y, \frac{1}{2}+z$. [c] The positions of the hydrogen atoms on the water molecules were not located. [d] The oxygen lies on a twofold axis, so two of the listed bonds are actually present.

Discussion

Geometry of the $[Ni(CN)_5]^{3-}$ Anion. The geometries of the three square-pyramidal $[Ni(CN)_5]^{3-}$ ions in the salts $[Cr(en)_3]_2[Ni(CN)_5]_2\cdot 3H_2O$, $[Cr(tn)_3][Ni(CN)_5]\cdot 2H_2O$, and $[Cr(NH_3)_6][Ni(CN)_5]\cdot 2H_2O$ substantially are identical. Their bond lengths and angles are compared in Table IX. The Ni-C-N angles for the cyanide ligands are all near 180°. These angles range from 175.6 (1.0) to 178.8 (9)° in the $[Cr(tn)_3]^{3+}$ salt and from 175.2 (6) to 178.2 (8)° in the $[Cr(NH_3)_6]^{3+}$ salt. The distortions from linearity are probably an effect of the torque exerted by hydrogen bonding.

The only deviation from general geometric agreement among the three square-pyramidal anions is the poor agreement among the very long and weak axial Ni-C bond lengths. For the three salts, the Ni-C distances found are 2.168 (14), 2.140 (10), and 2.101 (9) Å. The Ni-C bond distances are susceptible to apparent changes caused by the effects of thermal motion, although not through a mechanism explained by either the riding or the independent models.[20] A salient feature of the $[Ni(CN)_5]^{3-}$ ion in the $[Cr(en)_3]^{3+}$[3]

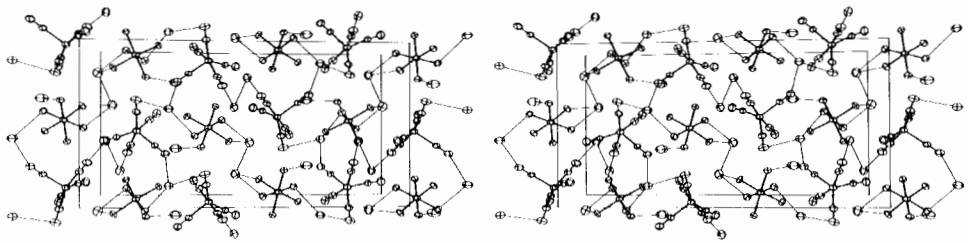

Figure 7. A stereoscopic packing diagram of the *xz* plane of $[Cr(NH_3)_6][Ni(CN)_5]\cdot 2H_2O$. The long axis is in the *x* direction. Only the water hydrogen bonds are illustrated.

Table XIX. Comparison of the Geometries of 1,3-Propanediamine Chelate Rings[a]

Compd	Conform	Distance, Å			Bond angle, deg			Dihedral angle,[b] deg			Torsional angle,[c] deg			Ref
		M–N	N–C	C–C	N–M–N	M–N–C	N–C–C	C–C–C	D_1	D_2	N–MN–C	M–NC–C	N–CC–C	
(−)D-$[Co(tn)_3]Br_3\cdot H_2O$	Δppp													*d*
Ring 1		2.00	1.46	1.54	96.0	117.5	112.0	114.0	31.1	58.1	35.2	51.9	71.9	
Ring 2		2.00	1.475	1.54	92.0	118.5	112.0	114.0	37.9	58.0	45.7	59.9	69.6	
Ring 3		2.00	1.46	1.545	95.0	116.5	113.0	114.0	34.0	61.5	40.3	48.0	65.2	
$[Cr(tn)_3][Ni(CN)_5]\cdot 2H_2O$	Δpδa													
Ring p		2.092	1.496	1.500	89.39	121.00	111.98	114.66	29.3	61.2	32.3	53.4	69.8	
Ring a		2.097	1.494	1.503	90.58	120.43	112.82	114.20	27.8	61.0	34.5	54.6	69.4	
Ring δ		2.100	1.472	1.462	89.21	116.59	119.18	117.20			26.6	61.2	32.9	
cis-$[Co(tn)_2(CO_3)]ClO_4$	Δpa													*e*
Ring A		1.97	1.485	1.51	91.9	120.7	110.0	113.8	32.6	61.5	38.6	56.7	68.7	
Ring B		1.945	1.50	1.49	89.7	116.6	111.1	112.7	43.7	58.5	50.4	63.6	65.6	
trans-$[Co(NO_3)_2(tn)_2]NO_3$		1.990	1.514	1.540	87.7	119.0	109.9	113.3	41.0	59.0	50.9	63.8	64.2	*f*
$[CoCl_2(tn)_2]Cl\cdot HCl\cdot 2H_2O$		2.00	1.46	1.54	95.4	119.1	114.6	111.3						*g*
$[Cu(tn)_2]SO_4\cdot H_2O$														*h*
Ring 1		2.03	1.49	1.50	93.2	122.5	113.1	114.2	19.5	59.7	23.0	46.4	68.2	
Ring 2		2.02	1.47	1.49	94.3	120.9	112.7	114.1	20.4	61.9	23.6	47.4	70.8	
$[Cu(tn)_2]SeO_4\cdot H_2O$														*h*
Ring 1		2.02	1.48	1.51	93.2	121.8	112.8	112.8						
Ring 2		2.03	1.49	1.51	93.5	121.5	110.2	113.1	22.3	65.7	26.1	50.1	73.9	
$[Cu(tn)_2](NO_2)_2$		2.038	1.494	1.520	86.8	115.8	111.6	115.0	47.5	54.9	54.7	65.0	62.3	*i*
$[Cu(tn)_2](NO_3)_2$		2.065	1.495	1.535	94.9	119.6	110.8	112.0	22.2	66.8	25.3	50.4	75.8	*j*
$[Ni(tn)_2(H_2O)_2](NO_3)_2$		2.095	1.529	1.512	92.9	121.3	110.1	115.1	21.4	69.4	24.9	53.3	78.1	*k*
$[Ni(tn)_2(H_2O)_2](ClO_4)_2$		2.113	1.484	1.515	87.9	118.4	111.7	116.0	38.1	59.7	44.2	59.9	67.2	*l*

[a] All bond lengths and angles represent average values within the individual ring. The dihedral and torsional angles have been calculated from reported fractional coordinates and cell data whenever possible. [b] The average dihedral angle between the NMN and NCCN planes is D_1. The average dihedral angle between the CCC and NCCN planes is D_2. [c] These are torsional angles as defined by J. D. Dunitz, *J. Chem. Educ.*, 47, 488 (1970). [d] References 37 and 38. [e] Reference 33. [f] E. Yasaki, I. Oonishi, H. Kawaguchi, S. Kawaguchi, and Y. Komiyama, *Bull. Chem. Soc. Jap.*, 43, 1354 (1970). [g] K. Matsumoto, S. Ooi, and H. Kuroya, *ibid.*, 43, 1903 (1970). [h] B. Morosin and J. Howatson, *Acta Crystallogr., Sect. B*, 26, 2062 (1970). [i] A. Pajunen and I. Belinskij, *Suom. Kemistilehti B*, 43, 70 (1970). [j] A. Pajunen, *ibid.*, 42, 15 (1969). [k] A. Pajunen, *ibid.*, 41, 232 (1968). [l] A. Pajunen, *ibid.*, 42, 397 (1969).

and $[Cr(tn)_3]^{3+}$ salts (Figure 1) is the anisotropy of the thermal motion in the cyanide groups. The primary axes for the thermal ellipsoids of the cyanide carbon atoms are oriented along the bond direction and those of the nitrogen atom thermal ellipsoids are perpendicular to the bond. This type of motion, probably a libration of the cyanide group and significantly anharmonic, is common among structures containing cyanide,[21-23] carbonyl,[24-27] or nitrosyl[28,29] groups. In the $[Cr(NH_3)_6]^{3+}$ salt (Figure 5) the thermal motion of the axial cyanide is much less than that of the axial cyanide groups in the other salts. For this reason the apical Ni-C distance in the $[Cr(NH_3)_6]^{3+}$ salt would be expected to exhibit a more accurate Ni-C bond length.

The energy differences between the more stable geometries of five-coordinate complexes are believed to be small. This is established in several systems by nuclear magnetic resonance studies[30] and in the solid state for the $[Ni(CN)_5]^{3-}$ anion by the observation of two distinct geometries in $[Cr(en)_3]_2[Ni(CN)_5]_2 \cdot 3H_2O$.[3] However, the equal stability of the two forms of $[Ni(CN)_5]^{3-}$ reveals nothing about the potential energy surface connecting them. If this surface is relatively flat, there is little or no potential barrier to an interconversion of the square-pyramidal and trigonal-bipyramidal forms and this rearrangement should be extremely facile. A relatively flat surface also implies extremely weak force constants for those vibrational modes which involve motion along the lowest energy path which connects the two geometries on the potential surface. The essentially constant geometry of the square-pyramidal $[Ni(CN)_5]^{3-}$ ion in three different lattice packing environments in three different salts implies a rigid structure. If the potential energy surface were flat in the region of the square-pyramidal geometry, the differences in the directions and strength of hydrogen bonds and of lattice packing forces would give rise to significant changes in bond parameters, especially bond angles. *Thus, although the square-pyramidal and trigonal-bipyramidal forms of the $[Ni(CN)_5]^{3-}$ anion differ in thermodynamic stability by only 1 or 2 kcal/mol, the kinetic energy barrier for this interconversion must be much greater than this.*

Although the details of the hydrogen bond structure surrounding each of the square pyramidal $[Ni(CN)_5]^{3-}$ ions is unique for each salt, there are some systematic features. The waters of crystallization in each structure link $[Ni(CN)_5]^{3-}$ anions related by an inversion center, twofold rotation, or glide plane. All of the cyanides of each anion participate in hydrogen bonding. Although each form of the anion in the $[Cr(en)_3]^{3+}$ salt participates in nine hydrogen bonds, the bonds formed to the square-pyramidal anion seem to be slightly stronger. The average N···N and O···N bonds are 3.03 and 2.90 Å for the square-pyramidal anion and 3.06 and 2.98 Å, respectively, for the distorted trigonal-bipyramidal form. There is little difference between the hydrogen bonding to the basal and apical cyanides.[3] Ten hydrogen bonds are formed to the $[Cr(tn)_3]^{3+}$ anion with average distances of 3.01 and 2.94 Å for the N···N and O···N bonds. The apical cyanide participates in several more hydrogen bonds than do the basal cyanide nitrogens. In the $[Cr(NH_3)_6]^{3+}$ salt, the anion participates in more hydrogen bonds than in the other two salts, but they are considerably weaker. The average N···N and O···N distances are 3.09 and 3.06 Å for the 12 hydrogen bonds and, again, the apical cyanide is somewhat favored in hydrogen bond formation.

The formation of systematically stronger and more extensive hydrogen bonding by the apical cyanides is consistent with the very weak bond formed by the axial cyanide anion and the nickel cation. The bonding in this square-pyramidal geometry of the complex may be approximated as an ion pair between CN^- and the square-planar $[Ni(CN)_4]^{2-}$ anion. In contrast, the trigonal-bipyramidal form of the $[Ni(CN)_5]^{3-}$ anion is isoelectronic, and nearly isostructural, with $Fe(CO)_5$. This emphasizes the differences in bonding between the two geometries and is consistent with the apparent preferential stabilization of the square-pyramidal geometry by extensive hydrogen bond formation.

Conformation of the $[Cr(tn)_3]^{3+}$ Cation. The overall configuration and conformation of the $[Cr(tn)_3]^{3+}$ ion is Λpδa.[31] Two of the rings are chair conformers and fold in a direction toward, rather than apart from, each other. The specific orientation of the chairs is designated by "a" and "p." The third ring has a δ chirality and is the first example of an isolated skew-boat conformer.

Mixed conformations in early energy-minimization studies were considered improbable in tris complexes.[32-34] Recently Hayes, Busch, and Parris[35] found that entropy effects favor the mixed conformation and significantly lower their calculated relative free energy. Niketic and Woldbye[36] found a mixed conformer, Λpaδ, to be the most stable conformation in calculations when using a "soft" nonbonded H-H function. However, no successful minimization calculation has been carried out on the Λpδa conformation. Because the nonbonded interactions between the chairs are very severe, the Λpδa conformation generally has been considered to be sterically impossible.

Chair Conformers. The two 1,3-propanediamine rings with the chair conformation fold toward each other and are related by an approximate twofold molecular symmetry axis (Figures 2 and 3). Two chairs which are cis to one another have three possible spatial arrangements. Only two of the conformations have previously been observed in crystal structures. The chair conformers in $[Co(tn)_3]Br_3 \cdot H_2O$[37,38] and in *cis*-$[Co(tn)_2CO_3]ClO_4$[33] all fold in the same rotational direction, showing Λpp arrangement. In *cis*-$[Co(tn)_2(NCS)_2][Sb(+)$-

(20) W. R. Busing and H. A. Levy, *Acta Crystallogr.*, 17, 142 (1964).
(21) K. N. Raymond and J. A. Ibers, *Inorg. Chem.*, 7, 2333 (1968).
(22) J. L. Hoard, T. A. Hamor, and M. D. Glick, *J. Amer. Chem. Soc.*, 90, 3177 (1968).
(23) J. K. Stalick and J. A. Ibers, *Inorg. Chem.*, 8, 1084 (1969).
(24) M. Elder and D. Hall, *Inorg. Chem.*, 8, 1268 (1969).
(25) M. Elder, *Inorg. Chem.*, 8, 2703 (1970).
(26) L. J. Guggenberger, *Inorg. Chem.*, 9, 37 (1970).
(27) M. R. Churchill and J. Wormald, *Inorg. Chem.*, 9, 2239 (1970).
(28) B. A. Frenz, J. H. Enemark, and J. A. Ibers, *Inorg. Chem.*, 8, 1288 (1969).
(29) D. M. P. Mingos and J. A. Ibers, *Inorg. Chem.*, 9, 1105 (1970).
(30) E. L. Muetterties, *Accounts Chem. Res.*, 3, 266 (1970), and references therein.
(31) F. A. Jurnak and K. N. Raymond, *Inorg. Chem.*, 11, 3149 (1972).
(32) F. Woldbye, "Studies on Optical Activity," Polyteknish Forlag, Copenhagen, 1969, p 210.
(33) R. J. Gene and M. R. Snow, *J. Chem. Soc. A*, 19, 2981 (1971).
(34) J. R. Gollogly and C. J. Hawkins, *Inorg. Chem.*, 11, 156 (1972).
(35) (a) L. J. De Hayes, M. Parris, and D. Busch, private communication. (b) L. J. De Hayes, Doctoral Thesis, The Ohio State University, 1971. (c) For a recent analysis of intra-ring strain for isolated six-membered chelate rings see L. J. De Hayes and D. H. Busch, *Inorg. Chem.*, 12, 1505 (1973).
(36) S. R. Niketic and F. Woldbye, private communication.
(37) Y. Saito, T. Nomura, and F. Marumo, *Bull. Chem. Soc. Jap.*, 41, 530 (1967).
(38) T. Nomura, F. Marumo, and Y. Saito, *Bull. Chem. Soc. Jap.*, 42, 1016 (1969).

tart]·$2H_2O$[39] the chairs have the Λpa conformation and fold apart from one another. The $[Cr(tn)_3]^{3+}$ cation is the first example in which the chairs fold into one another (the Λap conformation). In the absence of geometric distortions, the nonbonded interactions between the two chairs in the latter arrangement are severe. Snow has calculated[33] that the Λap conformer is energetically less stable than the Λpa and the Λpp conformations by 5.8 and 4.2 kcal/mol, respectively. The calculations also indicate that a pronounced flattening of one ring in the Λpp conformer and of two rings in the Λap conformer should occur to relieve the nonbonded interactions between the amine and methylene hydrogens of neighboring rings. We observe such a flattening in both chair conformers in $[Cr(tn)_3]^{3+}$. The average dihedral angles (Table XVIII)[17] between the NCCN and NCrN planes are 27.8 and 29.3° for the "a" and "p" chelate rings.

In addition to the degree of flattening, the two chair geometries are similar. The N-Cr-N angles are 90.6 and 89.4° and the average Cr-N-C angles are 120.4 and 121.0° for the "a" and "p" chairs, respectively. The remaining internal average N-C-C angles and C-C-C angle are 112.8 and 114.2° for the "a" chelate and 112.0 and 114.7° for the "p" conformer. Of greater significance than the individual similarities is the fact that the chairs in $[Cr(tn)_3]^{3+}$ conform favorably to general geometric trends observed in other chair structures.

The most puzzling feature of the geometry of the chair conformation is the wide variation of the N-M-N angle in chelates with the same M-N bond distance. We suggest that two parameters are of prime importance in affecting the resultant internal ring geometry. The first is the M-N bond length and the second is the dihedral angle, D_1, between the NMN and the NCCN planes.

A comparison of chair chelate geometries in Table XIX reveals the dependence of the N-M-N angle upon the M-N length. *In chairs with the same dihedral angle D_1, the N-M-N angle decreases as the M-N bond distance increases.* The two chair conformers of the $[Cr(tn)_3]^{3+}$ cation can be compared to ring 1 in the $[Co(tn)_3]^{3+}$ complex.[37,38] The Co-N bond of 2.0 Å is shorter than the average Cr-N bond of 2.096 Å. As predicted, the average N-Cr-N angle of 90.0° is smaller than the N-Co-N angle of 96°. A similar relationship between the M-N bond length and the N-M-N angle has been observed in five-membered chelate rings and is commonly referred to as the "chelate bite" effect. The conditional requirement of equivalent dihedral angles is not necessary in the five-membered ring due to the nature of the out-of-plane puckering.

The second type of distortion of the N-M-N angle is due to flattening of the NCCN fragment into the NMN plane. *In chairs with the same M-N bond distance, the N-M-N angle increases as the dihedral angle D_1 decreases.* The chair conformers in the $[Cr(tn)_3]^{3+}$ cation can be compared to the rings in $[Ni(tn)_2(H_2O)_2](ClO_4)_3$[40] and $[Ni(tn)_2(H_2O)_2](NO_3)_2$.[41] The dihedral angles D_1 in the $[Cr(tn)_3]^{3+}$ cation are 27.8 and 29.3° for rings "a" and "p." The respective N-Cr-N angles are 90.6 and 89.4°. As the dihedral angle D_1 increases to 38.1° in the chair conformer in $[Ni(tn)_2(H_2O)_2](ClO_4)_2$, the N-Ni-N angle decreases to 87.9°. In $[Ni(tn)_2(H_2O)_2](NO_3)_2$, the dihedral angle D_1 of the chair decreases to 21.4° and the N-Ni-N angle increases to 92.9°. The expansion of angles due to flattening is direct: as an equal-sided chair ring flattens into a planar hexagon, the internal angles increase from 109.5 to 120°. In metal chelate rings, only half of the chair conformer flattens, the NCCN fragment onto the NMN plane, and only three angles expand. This effect previously has not been considered.

In the absence of the flattening distortion, the N-M-N angles of the chair chelates are similar to the N-M-N angles found in five-membered rings. In ideal rings of both sizes, the remaining internal angles approach the tetrahedral angle. The torsional angles are 60° in the ideal rings and the closest NN and NC nonbonded interactions are similar.[42]

In the absence of nonbonded intramolecular interactions, the dihedral angle D_1 decreases as the M-N bond length increases. An undistorted chair can only be formed with minimum strain if the M-N bonds are short; with very long M-N bonds, the least strained chair conformation is flattened. Previously, flattening of the chair ring has been attributed to only a minimization of nonbonded interactions between the amine and methylene hydrogens of neighboring rings. We suggest that the length of the M-N bond also influences the degree of flatness in the chair. The correlation between the M-N bond length and the dihedral angle accounts for the trend among 1,3-propanediamine structures. The least flattened chairs are found among the rings with the shortest M-N bond length. In the $[Cr(tn)_3]^{3+}$ cation, the average M-N bond length for the chairs is 2.096 Å. Both chairs have flattened to an average dihedral angle D_1 of 28.5°.[45] It is difficult to determine whether the chair conformers flattened to minimize the extreme nonbonded replusions due to their unusual orientation or *vice versa*. The latter relation accounts for the occurrence of the skew-boat conformer. The hydrogen-bonding environment about each of the conformers is similar, indicating that there is little energy difference between a flattened chair and a skew-boat ring. Other isolated skew-boat conformers will probably occur in chelate systems with long M-N bonds.

Skew-Boat Conformer. It is clear from stereoscopic drawings and torsional angles (Table XIX) that the third ring forms the conformationally less stable twist or skew-boat conformer. The average dihedral angles of 79.0° between the $Cr-N_5-C_5$ and $N_6-C_6-C_{5-6}$ and between the $Cr-N_6-C_6$ and $N_5-C_5-C_{5-6}$ planes define the amount of twist present in the ring.

The most striking feature of the conformer is the much greater thermal motion in the carbon atoms of the skew-boat conformer relative to the other chair conformers

(39) K. Matsumoto, M. Yonezawa, H. Kuroya, H. Kawaguchi, and S. Kawaguchi, *Bull. Chem. Soc. Jap.*, 43, 1269 (1970).
(40) A. Pajunen, *Suom. Kemistilehti B*, 42, 397 (1969).
(41) A. Pajunen, *Suom. Kemistilehti B*, 41, 232 (1968).

(42) The chair conformer in $[Cu(tn)_2](NO_2)_2$[43] is only slightly distorted; the dihedral angle D_1 is 47.5°. The average Cu-N bond of 2.038 Å and the N-Cu-N angle of 86.8° compare favorably to the five-membered ring in $[Cu(en)_2](NO_3)_2$.[44] The ethylenediamine chelate has a N-Cu-N angle of 86.2° and an average Cu-N bond distance of 2.028 Å.
(43) A. Pajunen and I. Belinskij, *Suom. Kemistilehti B*, 43, 70 (1970).
(44) Y. Komiyama and E. C. Lingafelter, *Acta Crystallogr., Sect. B*, 17, 1145 (1964).
(45) The flattening mode about the M-N-C angles also affects the remaining ring geometry, especially the puckering of the CCC plane. As the ring flattens about the M-N-C angle, the torsional angle about the N-C bond decreases, and the amine hydrogens effectively rotate. To minimize nonbonded repulsions, the methylene hydrogens rotate in the same direction as neighboring amine hydrogens. The rotation results in an increase in the torsional angles about the C-C bond. Furthermore, a comparison of the 1,3-propanediamine chelates indicates that the torsional distortion is the same or greater about the C-C bond in most structures than about the N-C bond. The equal or smaller torsional distortion about the N-C bond implies that the torsional energy barrier is the same or greater for the N-C bond than for the C-C bond. The contrary assumption has been applied in most energy-minimization calculations.

(Figure 3). This motion is primarily perpendicular to the plane formed by the two C-N or C-C bonds for each atom. The thermal motion observed is consistent with two expectations. First, within a ring the thermal motion should be much less for the nitrogen atoms, since these are bound firmly to a heavy, fixed chromium atom. Motion perpendicular to planes of the bonds is then easiest at the central carbon atom, the ring atom farthest from the chromium atom. The second expectation is that the chair conformation is relatively rigid and should exhibit less thermal motion than the more flexible twist form. This observation can be seen easily from an examination of conformational models of cyclohexane. In fact, the twist form of cyclohexane is so flexible that recent calculations indicate it undergoes virtually free pseudorotation at room temperature.[46] It is impossible in this case for the twist conformer actually to pseudorotate since this would involve moving the entire $[Cr(tn)_3]^{3+}$ cation within the crystal lattice array. However, the observed thermal motion is of the type which would give rise to pseudorotation in the absence of this constraint. The observed thermal motion attributed to pseudorotation should not be confused with ring disorder resulting from an equilibrium mixture of the two possible chair conformers "p" and "a," within the same ring. Both phenomena would result in large carbon thermal ellipsoids. However, the carbon atom positions relative to one another would differ depending upon the phenomenon: disorder or pseudorotation. If disorder of the ring occurred, the C-N bonds would lie in the same plane, not form an angle with one another as they do in the present structure. An example of the latter type of thermal motion is found in two of the five-membered rings in (+)D-$[Co(en)_3]Cl_3 \cdot H_2O$,[47,48] in which the structure analysis reveals large carbon thermal ellipsoids with primary axes perpendicular to the bonds in the ethylenediamine rings.

From the geometric data in Table XII, the skew-boat conformer appears to be a flattened ring. All internal angles except the N-M-N angle are considerably expanded. The average Cr-N-C, N-C-C, and C-C-C angles are 116.6, 119.2, and 117.2°. However, it is difficult to estimate the extent to which angular distortions are due to a time-average effect of the thermal motion. If the angular distortions are real, the flattening mode and its geometric effects upon the skew-boat conformer are expected to be different from that in the chair. The probable reasons for chair flattening, such as nonbonded interactions with the methylene hydrogens, do not exist in the skew-boat conformer in the $[Cr(tn)_3]^{3+}$ ion.

The distances and appropriate angles for the hydrogen bonds to the amine protons are listed in Table XIII. The "p" chair and the skew-boat conformer each form three hydrogen bonds. The remaining "a" chair forms only two hydrogen bonds. Atom CrN_6 in the skew-boat conformer shares NiN_4 with CrN_2, CrN_5 forms two bonds, sharing NiN_1 with CrN_2 and NiN_5 with CrN_3. In the "a" chelate CrN_2 forms two bonds with NiN_1 and NiN_4, and CrN_1 bonds to O_2. Each amine in the "p" chelate forms one hydrogen bond, CrN_3 to NiN_5 and CrN_4 to O_1. We conclude that the energy differences between the flattened chair rings and the skew-boat conformer must be exceedingly small.

(46) H. M. Pickett and H. L. Strauss, *J. Amer. Chem. Soc.*, **92**, 7281 (1970).
(47) Y. Saito, *Pure Appl. Chem.*, 17, 21 (1968).
(48) M. Iwata, K. Nakatsu, and Y. Saito, *Acta Crystallogr., Sect. B*, 25, 2562 (1969).

Effect of Crystal Decomposition. A significant decomposition of the crystal in the primary X-ray beam (as measured by a diminution of diffracted intensities with exposure) occurs for a high percentage of structure analyses. It is therefore of some interest to compare the structure results derived from the low-temperature data set, in which negligible decomposition occurred, and the room-temperature data set, in which the final intensities of standards had dropped to 14% of their initial values.

Given the known formation constant and approximate solubility data of the $[Ni(CN)_5]^{3-}$ salts, it seems highly likely that all of the crystalline salts which have been isolated are thermodynamically unstable at room temperature. All of the crystals at room temperature are then probably metastable and the rapid decomposition in the X-ray beam may be due to its acceleration of the phase transition. The change with temperature is dramatic: crystals of $[Cr(NH_3)_6][Ni(CN)_5] \cdot 2H_2O$ decompose completely in an X-ray beam within 1–2 hr at room temperature but are indefinitely stable at −10°.

The final structure results for the room-temperature data set (23°, 2630 reflections with $F^2 > \sigma(F^2)$, $R_w = 8.3\%$) of $[Cr(tn)_3][Ni(CN)_5] \cdot 2H_2O$ are given in Tables XX and XXI.[17] A comparison with the low-temperature results described earlier (−80 (2)°, 1671 reflections with $F^2 > 3\sigma(F^2)$, $R_w = 5.4\%$) indicates that the important features of the structure are invariant. The relative thermal motion of the skew-boat ring is much larger than in the chairs in both data sets. As expected, the magnitude of the thermal ellipsoids is smaller for the low-temperature data set. The packing environment is not significantly different. An additional hydrogen bond from a water molecule to the cation is found in the low-temperature structure. The only significant differences between the structures occur in the ring parameters. The N-C and C-C bond lengths have refined to more reasonable values using the low-temperature data. Several internal ring angles, notably N-C-C and the C-C-C, shifted significantly. We conclude that fairly reliable structural information can be obtained from data which have been corrected for very large isotropic decomposition, where by isotropic we mean the relative intensities of all reflections do not change significantly during crystal decomposition.

Acknowledgment. We gratefully acknowledge the financial support of the National Science Foundation (through Grants GP-29764, GP-36977X, and GP-10510). We thank the University of California Computing Center for the use of subsidized computing time.

Registry No. $[Cr(tn)_3][Ni(CN)_5] \cdot 2H_2O$, 52154-76-4; $[Cr(NH_3)_6][Ni(CN)_5] \cdot 2H_2O$, 52154-78-6.

Supplementary Material Available. Figure 6, showing a perspective view down the pseudo-threefold axis of the $[Cr(NH_3)_6]^{3+}$ cation, and Tables III, V, VI, VIII, XI, XV, XVI, XVIII, XX, and XXI, showing structure factor amplitudes, positional parameters for hydrogen atoms, and best weighted least-squares planes for $[Cr(NH_3)_6][Ni(CN)_5] \cdot 2H_2O$ and $[Cr(tn)_3][Ni(CN)_5] \cdot 2H_2O$, bond distances and angles for $[Cr(NH_3)_6]^{3+}$, dihedral angles in the 1,3-propanediamine rings of $[Cr(tn)_3]^{3+}$, and bond distances and angles and rms amplitudes of vibration for $[Cr(tn)_3][Ni(CN)_5] \cdot 2H_2O$, will appear following these pages in the microfilm edition of this volume of the journal. Photocopies of the supplementary material from this paper only or microfiche (105 × 148 mm, 24× reduction, negatives) containing all of the supplementary material for the papers in this issue may be obtained from the Journals Department, American Chemical Society, 1155 16th St., N.W., Washington, D. C. 20036. Remit check or money order for $5.00 for photocopy or $2.00 for microfiche, referring to code number INORG-74-2387.